Epithelial-to-Mesenchymal Transition and its Association with PD-L1 and CD8 T cells in Thyroid Cancer

Marra Aghajani (marra.aghajani1@gmail.com)
Western Sydney University
Tao Yang
Sydpath
Ulf Schmitz
Centenary Institute
Alexander James
Ingham Institute
Charles Eugenio McCafferty
Western Sydney University
Paul de Souza
Western Sydney University
Navin Niles
Western Sydney University
Tara Roberts
Western Sydney University

Research

Keywords: thyroid cancer, epithelial-to-mesenchymal transition, programmed cell death-ligand 1, CD8, survival

Posted Date: June 10th, 2020

DOI: https://doi.org/10.21203/rs.3.rs-34509/v1

Epithelial-to-Mesenchymal Transition and its Association with PD-L1 and CD8 T cells in Thyroid Cancer

Marra Jai Aghajani[a,b] BMedRes

Tao Yang[b,c,d] MBBS MSc PhD FRCPA

Ulf Schmitz [e,f,g] Dipl.-Ing. (FH) PhD (Dr.-Ing.)

Alexander James[a] BSc (HonsI), PhD

Charles Eugenio McCafferty[a,b] BMedRes

Paul de Souza [a,b,k] BSc (Med), MBBS, MPH, PhD, FRACP

Navin Niles[a,b,i,j] BSc. (Med.) MBBS FRACS

Tara L. Roberts[a,b,h] BSc (HonsI), PhD

[a]Ingham Institute for Applied Medical Research, Liverpool, NSW, Australia

[b]School of Medicine, Western Sydney University, Campbelltown, NSW, Australia

[c]Saint Vincent's Clinical School, UNSW Sydney, Sydney, Australia

[d]SydPath, Saint Vincent's Hospital, Sydney, Australia

[e]Computational BioMedicine Laboratory Centenary Institute, The University of Sydney, Australia

[f]Gene & Stem Cell Therapy Program Centenary Institute, The University of Sydney, Australia

[g]Faculty of Medicine & Health, The University of Sydney, Australia

[h]South West Sydney Clinical School, UNSW Sydney, Sydney, Australia

[i]Department of Head & Neck Surgery, Liverpool Hospital, Liverpool, NSW, Australia

[j]Department of Clinical Medicine, Faculty of Medicine and Health Sciences, Macquarie University, Sydney, Australia

[k]School of Medicine, University of Wollongong, NSW, Australia

Marra Jai Aghajani

Mobile: 0411743201

Email: marra.aghajani1@gmail.com

Tao Yang

Mobile: 0412884118

Email: tao.yang@svha.org.au

Ulf Schmitz

Mobile: +61 2 9565 6209

Email: u.schmitz@centenary.org.au

Alexander James

Email: alexander.james@unsw.edu.au

Charles Eugenio McCafferty

Mobile: 0499777181

Email: c.mccafferty@westernsydney.edu.au

Paul de Souza

Mobile: 0404003220

Email: p.desouza@westernsydney.edu.au

Navin Niles

Mobile: 0416229519

Email: navinniles@me.com

Tara Roberts

Mobile: 0410565770

Email: Tara.Roberts@westernsydney.edu.au

Name of corresponding author: Marra Aghajani

Address of corresponding author: 1 Campbell St, Liverpool NSW 2170

Running title: EMT, PD-L1 and CD8 as Thyroid Cancer Biomarkers

Abstract:

Background: Programmed cell death-ligand 1 (PD-L1) has recently been shown to play a role in the regulation of epithelial-to-mesenchymal transition (EMT) in some cancers. However, the relationship between PD-L1 expression, EMT and the inflammatory tumour microenvironment has yet to be investigated in thyroid cancer.

Methods: To address this issue, we examined the expression of CD8, PD-L1 and the EMT markers E-cadherin and vimentin in a cohort of papillary thyroid cancer (PTC) patients and investigated the association of these with clinicopathologic characteristics and disease-free survival (DFS). CD8 T cells, PD-L1 and EMT status was assessed in 74 patients with PTC via immunohistochemistry (IHC). The relationship between PD-L1 and EMT was further investigated in three thyroid cancer cell lines (8505C, K1 and FTC-133) via western blot and live cell imaging In order to expand our *in vitro* findings, the normalised gene expression profiles of 516 thyroid cancer patients were retrieved from The Cancer Genome Atlas (TCGA). An EMT score of each thyroid cancer sample was calculated and correlated with PD-L1 gene expression, or the mean expression of IFN signature genes.

Results: PD-L1 positivity was significantly higher in PTC patients exhibiting a mesenchymal phenotype ($p = 0.012$). Kaplan-Meier analysis revealed that PD-L1 ($p = 0.045$), CD8 ($p = 0.038$) and EMT status ($p = 0.038$) were all significant predictors for DFS. Sub-analysis confirmed that the poorest DFS was evident in PD-L1 positive patients with EMT features and negative CD8 expression ($p < 0.0001$). IFN-γ

treatment induced upregulation of PD-L1 and significantly promoted an EMT phenotype in two thyroid cancer cell lines.

Conclusions: Our findings suggest that PD-L1 signalling may play a role in stimulating EMT in thyroid cancer. EMT, CD8 and PD-L1 expression may serve as valuable predictive biomarkers in patients with PTC. The combination of EMT inhibitors with immunotherapies targeting the PD-1/PD-L1 axis may be beneficial in cancer patients with mesenchymal metastatic thyroid cancers.

Keywords: thyroid cancer, epithelial-to-mesenchymal transition, programmed cell death-ligand 1, CD8, survival

Introduction:

The incidence rate of thyroid cancer has risen rapidly over the last four decades (1). Differentiated thyroid cancers (DTCs), derived from thyroid follicular cells, are the most common subtype, accounting for over 90% of all newly diagnosed cases (2). The mounting incidence rate has been attributed to improvements in access to health care systems, increased incidental detection on imaging, more widespread diagnostic testing of asymptomatic thyroid nodules, a rise in the volume and extent of surgery, and modifications in pathology practices (3). However, recent evidence supports a true increase in the occurrence of the disease, possibly due to hormonal, environmental, and genetic factors (4).

Whist the majority of patients with DTC have a favourable prognosis, 1 to 9% present with distant metastasis at the time of initial diagnosis (5), and 7 to 23% show distant metastasis during follow-up (6). Moreover, 25% to 50% of patients with locally advanced or metastatic DTC become refractory to radioactive iodine (RAI) therapy (7). Inoperable or RAI-refractory metastatic DTC is associated with a 10-year survival of only 10%, and restricted treatment options are currently available (7).

Following initial surgery, the American Joint Committee on Cancer (AJCC)/ International Union against Cancer (UICC) Tumour Node Metastasis (TNM) staging system is commonly implemented to predict disease-specific mortality and is consulted when tailoring decisions concerning postoperative adjunctive therapy. Whilst the AJCC/UICC TNM staging provides important information regarding mortality, it inaccurately predicts the risk of persistent or recurrent disease following

initial therapy (8). Research is needed to establish whether the inclusion of additional variables can enhance the predictive capabilities of the current AJCC/UICC TNM staging system.

Programmed cell death protein 1 (PD-1), an inhibitory costimulatory molecule expressed on activated T, B, and NK cells, plays a critical role in the regulation of peripheral tolerance (9). Two PD-1 binding ligands have been identified; programmed death ligand 1 (PD-L1) and programmed death ligand 2 (PD-L2) (10). PD-L1 is expressed by various human tumours and, following binding to PD-1, has been shown to induce potent inhibition of T-cell mediated anti-tumoural immunity (11). Elevated PD-L1 levels have been associated with a poor prognosis in multiple cancer types (12). We have completed a meta-analysis confirming that non-medullary thyroid cancer patients expressing PD-L1 were three times more likely to have a poorer disease-free survival (DFS) than patients who did not have positive PD-L1 expression (13). Immunotherapies targeting the PD-1/PD-L1 pathway have demonstrated durable responses in selected patients across multiple cancer types, including thyroid cancer (14, 15). However, optimal biomarkers predictive of patient response are currently lacking (16).

Epithelial-to-mesenchymal transition (EMT) is a biological process which plays a central role in cancer progression, metastasis, and drug resistance. During EMT, a polarised epithelial cell, which interacts with the basement membrane, adopts a mesenchymal cell phenotype, which is associated with an enhanced migratory capacity and invasiveness, greater resistance to apoptosis, and markedly increased production of extracellular matrix components (17). Throughout this

process, epithelial markers including epithelial cell adhesion molecule (EpCAM) and E-cadherin are down-regulated, whilst the mesenchymal markers vimentin and N-cadherin increase in expression. Vimentin has gained much importance as a canonical marker of EMT, with its overexpression associated with accelerated tumour growth, invasion, and poor prognosis (18). E-cadherin is a member of the cadherin family that is primarily detected in epithelial cells. Decreased E-cadherin expression reduces cell-cell contact and promotes EMT induction, resulting in tumour motility (18). Therefore, E-cadherin and vimentin are promising biomarkers associated with invasiveness, poor differentiation and malignant phenotype.

A bidirectional relationship has recently been established between EMT and PD-L1 expression (19-22). Preliminary observations point to a potential role of EMT markers as predictors of patient response to PD-1/PD-L1 axis therapies (21). Cancers containing a high level of pre-existing T cell infiltrate and a pro-inflammatory IFN signature, referred to as ‘hot’ tumours, have also been shown to more readily respond to PD-1/PD-L1 directed immunotherapies blockade (23). However, the relationship between T cell infiltrate, PD-L1 and EMT status, and their influence on the progression and metastasis of human thyroid cancer, has yet to be investigated. To address this issue, we examined the expression of CD8, PD-L1 and the EMT markers E-cadherin and vimentin in a cohort of PTC patients and investigated the association of these with clinicopathologic characteristics and DFS. The relationship between these markers were further investigated in three thyroid cancer cell lines via western blot and IncuCyte live cell imaging.

Methods:

Patient characteristics

Ethics approval was obtained from the South West Sydney Local Health District Human Research Ethics Committee via the Centre for Oncology Education and Research Translation (CONCERT) Biobank, Australia/TCRC/3/02- 03-2015 (24, 25). In this study, the archived paraffin embedded tissues from 74 PTC patients that underwent surgical resection within the South West Sydney Local Health District from 2006 to 2015 were obtained. Patient demographics and clinicopathologic parameters, including age, sex, tumour stage, tumour size, capsular invasion, extrathyroidal extension, lymphovascular invasion, multicentricity, presence of concurrent lymphocytic thyroiditis and lymph node metastasis, were acquired via retrospective medical record review. Standard American Joint Committee on Cancer, 8th edition, tumour-node-metastases (TNM) scoring was implemented for thyroid cancer staging. All patients were followed up for survival status until October 2019.

DFS was defined as the period between completion of primary treatment and detection of residual disease, recurrent disease or death. This definition was adopted from the 2015 American Thyroid Association (ATA) Management Guidelines (26). An excellent response (absence of persistent tumour) following initial therapy was defined as negative imaging and either a low serum thyroglobulin (Tg) during thyroid stimulating hormone (TSH) suppression (Tg <0.2 ng/mL) or following stimulation (Tg <1 ng/mL). A structural incomplete response was defined as structural or functional evidence of disease with any Tg level, whilst a biochemical incomplete response was

designated to patients with negative imaging and a suppressed Tg ≥1 ng/mL or a stimulated Tg ≥10 ng/mL. Patients that did not experience tumour recurrence were censored at the last follow-up contact.

Immunohistochemistry

Formalin-fixed paraffin-embedded (FFPE) tissues were collected from 74 patients with a confirmed diagnosis of PTC and were used to construct tissue microarrays (TMAs). Sections were stained with anti-PD-L1 (clone SP263) rabbit monoclonal primary antibody (Ventana Medical Systems) on the Ventana BenchMark Ultra automated staining platform using the OptiView Detection Kit. The Leica Bond III Immuno-autostainer was used for CD8 staining with the mouse anti-human CD8 clone C8/144B, 1:100 (DAKO). TMAs were also stained with the monoclonal mouse anti-human e-cadherin clone NCH-38, 1:100 (DAKO) and monoclonal mouse anti-vimentin clone V9, 1:500 (DAKO).

Vimentin staining was scored as follows: 0 = no expression, 1 = fragmented membranous and/or weak to moderate expression, 2 = fragmented strong or fully membranous moderate expression, and 3 = fully membranous strong expression. A score of ≥2 was considered as positive vimentin expression. The scoring for E-cadherin was based on the area intensity score method, which incorporates both the staining intensity and the number of positive cells. The intensity of staining was scored as 0 = negative, 1 = weak, 2 = moderate, and 3 = intense. The percentage of positively stained cells was scored as follows; 0 = 0-5% positive cells, 1 = 6-25% positive cells, 2= 26-50% positive cells, 3 = 51-75% positive cells, and 4 = 75-100% positive cells. The two scores for the intensity and the percentage of positive cells

were then multiplied to generate a final score ranging from 0-12. E-cadherin expression was dichotomised as negative (score of 0-6) and positive (score of 7-12) for outcome analyses. Patients considered to be EMT positive were those that were scored both vimentin “positive” and E-cadherin “negative”.

PD-L1 expression was scored based on the percentage of immunopositively stained cells, with a score of ≥1% considered positive PD-L1 staining. Scoring of CD8 expression was performed as previously described (27). Briefly, a quantitative score based on the percentage of immunopositively stained cells was given according to the following scale: 1 (<1% cells); 2 (1%-10% cells); 3 (11%-33% cells); 4 (34%-66% cells); and 5 (67%-100% cells). Staining intensity was then scored as follows: 0 (none), 1+ (mild), 2+ (moderate), and 3+ (intense). Finally, Allred scores (ranging from 1-8) were calculated by adding the percentage positivity scores and the intensity scores for each of the sections. The median value was used to separate the patient cohort into 2 groups with either negative or positive CD8 expression. Figure 1 provides representative cases of E-cadherin, vimentin, PD-L1 and CD8 scoring. Two authors (T.Y and M.A) blinded to tumour clinicopathological characteristics and patient outcomes scored the slides, with any discrepancies resolved by consensus.

Cell culture

The follicular thyroid cancer (FTC) and PTC cell lines FTC-133 and K1 were cultured in DMEM: Ham’s F12 (1:1) medium (Sigma-Aldrich) containing 2mM glutamine (Thermo Fisher) and 10% foetal bovine serum (FBS) (Thermo Fisher). The anaplastic thyroid cancer (ATC) cell line 8505C was cultured in EMEM (HBBS)

medium supplemented with 2mM glutamine (ThermoFisher), 1% non-essential amino acids (Sigma-Aldrich) and 10% FBS (Thermo Fisher). All media were supplemented with penicillin-streptomycin (Thermo Fisher) and all cells were incubated at 37°C in 5% CO_2. EMT was induced using recombinant human IFN-γ (300-02) (10ng/mL, Peprotech).

Live cell imaging assays were performed using the IncuCyte® Live-Cell Analysis System (Essen BioScience, Ann Arbor, MI, USA). Cells were imaged at 10X magnification at 37°C with 5% CO_2. Images were acquired every 4 hours for 48 hours.

Western blot analysis

Western blotting was performed as described previously (28). Briefly, cells were harvested and lysed in RIPA buffer supplemented with phosphatase (sodium fluoride, sodium molybdite, sodium pyrophosphate) and complete Mini, EDTA-free protease inhibitors (Roche, UK). 15-25 µg total protein (depending on different proteins) were separated by sodium-dodecyl sulfate-polyacrylamaide gel electrophoresis and then transferred to polyvinylidene difluoride membranes (Roche, UK). For each gel, the same amount of protein was loaded per lane. Membranes were then blocked in 5% non-fat milk in Tris-buffered saline-Tween for 1 hour. The immunoblotting was performed by incubation at 4°C overnight with the following primary antibodies: anti–PD-L1 antibody (13684) (Cell Signaling Technology, Boston, USA), anti–E-cadherin (ab15148) (Abcam), anti-vimentin (ab92547) (Abcam) and β-actin (Cell Signaling Technology, Danvers, MA, USA), which was used as an endogenous protein for normalisation. Blots were then washed and

incubated with a 1:1000 dilution of anti-Rabbit IgG H&L (HRP)-conjugated secondary (Cell Signaling Technology, Danvers, MA, USA) or a 1:1000 dilution of anti-Mouse IgG H&L (HRP)-conjugated secondary (Cell Signaling Technology, Danvers, MA, USA). Signals were detected by enhanced chemiluminescence Plus reagents (PerkinElmer) and images were captured using a Licor Odyssey System. Signal quantification was obtained using Image Studio Lite software (Version 5.2.5). All experiments were performed in triplicate.

Dataset analysis

Normalised gene expression profiles (RNA Seq V2 RSEM) of 516 PTC patients were retrieved from The Cancer Genome Atlas (TCGA) via the Cancer Genomics Data Server package (cgdsrv1.2.10; github.com/cBioPortal/cgdsr). The EMT score was computed using the mean expression of mesenchymal genes (ZEB1, ZEB2, SNAI1, SNAI2, TWIST1, TWIST2, VIM, FOXC2, SOX10, FN1, MMP2, MMP3) minus the mean expression of epithelial genes (CDH1, CLDN3, CLDN4, CLDN7, DSP) (22). Correlation coefficients of PD-L1 expression and EMT score, or mean expression of the IFN signature genes and EMT score were computed using Pearson correlation. Survival analyses (Kaplan-Meier) based on DFS were performed using the survival package (v2.44 1.1; github.com/therneau/survival). The heatmap was generated using the ComplexHeatmap package (v2.1.0) (29). All data analyses have been performed using R version 3.6.0.

Statistical analysis

Correlations were analysed using the Pearson's chi-squared test and Fisher's exact test. The student t-test was implemented to compare differences between

control and treated cell lines. Two-sided *p* values < 0.05 was considered statistically significant. Survival curves were plotted using the Kaplan-Meier method and compared using the log-rank test. A Cox regression model was used to perform multivariate analyses. All statistical analyses were completed using GraphPad Prism v.7.0d and SPSS software (version 22).

Results:

Patient characteristics

The main characteristics of the 74 PTC patients included in the study are detailed in Table 1. The median age of the patients at diagnosis was 51 years. The majority of patients were female (87.8%) or had a tumour size less than 2 cm (79.7%). Less than 15% of the cohort were diagnosed with TNM stage III/IV disease. This was expected as the majority of thyroid cancers are identified and diagnosed at an early stage.

Table 1: Clinical Summary of Patients**.**

Patient characteristics	Number of Patients (n = 74)	
Age		
Median [range]	51 [24-80]	
<55	44	59.5%
≥55	30	40.5%
Sex		
Male	9	12.2%
Female	65	87.8%
TNM stage		
I/II	64	86.5%
III/IV	10	13.5%
Tumour size		
<2 cm	59	79.7%
≥2 cm	15	20.3%
Multifocality		
Present	14	18.9%
Absent	60	81.1%
Extrathyroidal extension		
Present	15	20.3%
Absent	59	79.7%
Lymphovascular invasion		
Present	6	8.1%
Absent	68	91.9%
Lymph node metastases		
Present	14	18.9%
Absent	60	81.1%
Concurrent Hashimoto's Thyroiditis		
Present	30	40.5%
Absent	44	59.5%

PD-L1 expression is associated with EMT status in papillary thyroid cancer patients

The expression of E-cadherin, vimentin, PD-L1 and CD8 were all assessed via IHC staining of TMAs. Of the 74 cases, 16 (21.6%) were scored positive for E-cadherin whilst 51 (68.9%) patients expressed positive vimentin staining. Forty-five (60.8%) cases were considered EMT positive (E-cadherin^{negative} and vimentin^{positive}). Positive PD-L1 expression was observed in 49 patients (66.2%). PD-L1 positivity was significantly higher in PTC patients displaying a mesenchymal phenotype

(Figure 2; $p = 0.012$), as determined by negative E-cadherin and positive vimentin expression. Elevated CD8 levels were identified in 39 (52.7%) patients.

PD-L1, EMT and CD8 are predictive for DFS in PTC patients

EMT status and the expression of PD-L1, E-cadherin, vimentin, and thre presence of CD8 T cells were not significantly associated with any clinicopathological characteristics (Additional Files 1, 2, 3, 4 and 5). Interestingly, all six PTC patients which experienced lymphovascular invasion were EMT positive (i.e. displayed a mesenchymal phenotype); however, this did not reach statistical significance (Table 6; $p = 0.075$), likely due to the small number of patients in this sub-group.

At the time of analysis, the median duration of follow-up of the 74 cases was 45.5 months (range: 2-129 months). A total of 16 (21.6%) cases experienced tumour persistence and/or recurrence. Univariate analysis revealed that e-cadherin was not a significant predictor of DFS in our cohort (Figure 3A; $p = 0.384$); however, a positive vimentin score was significantly associated with a reduced DFS (Figure 3B; $p = 0.003$). A high density of tumoural CD8 T cells was a favourable biomarker predictive of improved DFS (Table 2, Figure 3C; $p = 0.028$), whilst positive PD-L1 expression was significantly associated with an increased incidence of persistent or recurrent disease (Table 2, Figure 3D; $p = 0.048$. The presence of lymph node metastases (Table 2; $p = 0.006$) and lymphovascular invasion ($p = 0.004$) were also significant predictors of DFS on univariate analysis in our cohort.

Table 2: Univariate and multivariate analysis of clinicopathologic factors associated with DFS in PTC cases.

Patient characteristics	Univariate analysis	Multivariate analysis		
	P value	HR	95% CI	P value
Age				
<55 vs. ≥55	0.736	1.986	0.546-7.226	0.298
Sex				
Male vs. Female	0.362	1.258	0.281-5.643	0.764
TNM stage				
I vs. II vs. III vs. IV	0.061	1.043	0.488-2.231	0.913
Tumour size				
<2 cm vs. ≥2 cm	0.327	0.956	0.253-3.608	0.947
Multifocality				
Present vs. Absent	0.128	2.340	0.604-9.063	0.219
Extrathyroidal extension				
Present vs. Absent	0.154	1.050	0.260-4.241	0.945
Lymphovascular invasion				
Present vs. Absent	**0.004***	2.826	0.416-19.188	0.288
Lymph node metastases				
Present vs. Absent	**0.006***	1.819	0.441-7.515	0.408
Concurrent Hashimoto's Thyroiditis				
Present vs. Absent	0.424	0.900	0.242-3.346	0.875
PD-L1				
Negative vs. Positive	**0.048***	3.053	0.599-15.552	0.179
CD8				
Negative vs. Positive	**0.028***	0.536	0.135-2.130	0.376
EMT status				
$E\text{-}cad^{neg}/Vim^{neg}$ vs. $E\text{-}cad^{neg}/Vim^{pos}$ vs. $E\text{-}cad^{pos}/Vim^{neg}$ vs. $E\text{-}cad^{pos}/Vim^{pos}$	**0.026***	3.132	1.102-8.897	**0.032***

Subgroup analysis

Based on EMT marker staining, we categorised all 74 tissue sections into four subgroups; 1) E-cadherin^{negative}/vimentin^{negative} (n=13), 2) E-cadherin^{negative}/vimentin^{positive} (n=45), 3) E-cadherin^{positive}/ vimentin^{negative} (n=10), 4) E-cadherin^{positive}/vimentin^{positive} (n=6). Patients that were E-cadherin^{negative}/ vimentin^{positive} and E-cadherin^{positive}/vimentin^{positive} experienced the shortest DFS compared to the other two subgroups (Figure 4A; $p = 0.026$). The patients were then allocated one of two major subgroups; 1) an EMT positive subgroup (n=45), including patients with a negative E-cadherin and positive vimentin scores, or 2) an EMT negative subgroup (n=29), which included all other patients. EMT positive cases had a significantly higher incidence of recurrence compared to EMT negative patients ($p = 0.021$). On multivariate analyses, EMT status remained as the only significant independent predictor for DFS (Table 2; $p = 0.032$).

Further sub-analysis was performed to assess the relationship between PD-L1, EMT and CD8 expression, and prognosis. Patients that were scored both EMT and PD-L1 negative (n=39) had the longest DFS compared with all other patients (n=34) (Figure 4B; $p = 0.003$). Moreover, PD-L1^{negative}/EMT^{negative}/CD8^{positive} patients (n=7) experienced no recurrent or persistent disease, whilst those considered PD-L1^{positive}/EMT^{positive}/CD8^{negative} (n=15) experienced the shortest DFS (Figure 4C; $p < 0.0001$).

<u>Clinical datasets and mRNA expression profiles</u>

In order to expand our IHC findings, the normalised gene expression profiles of 516 thyroid cancer patients were retrieved from The Cancer Genome Atlas (TCGA). The profiles were comprised of 399 PTCs, 107 FTCs, 1 patient with PDTC,

1 patient with well-differentiated thyroid cancer, and 8 thyroid cancers that were not otherwise specified. An EMT score of each thyroid cancer sample was calculated using the mean expression of mesenchymal genes minus the mean expression of epithelial genes (additional detail in Methods section). This was then correlated with PD-L1 gene expression, or the mean expression of IFN signature genes (Figure 5F). We observed a moderate positive linear relationship between EMT status and PD-L1 expression (Figure 5A; r = 0.481171) and an IFN gene signature (Figure 5B; r = 0.360384). When considering only PTCs (n=399), the correlation coefficient between EMT status and PD-L1 strengthened (Figure 5C; r = 0.502354). Moreover, in the subset of PTCs which experienced disease recurrence/progression (n=40), a strong correlation was identified between positive PD-L1 and EMT expression (Figure 5D; r = 0.623002). This was also observed when patients of all subtypes which experienced disease recurrence/progression (n=49) were included (Figure 5E; r = 0.656826). These results align with the findings from our patient cohort, in which we observed a significant association between PD-L1 expression and EMT status. In the TCGA PTC patient cohort, a higher EMT and mesenchymal genes score were both significantly associated with poorer DFS outcomes (p = 0.0027 (Figure 5G) and p = 0.0085 (Figure 5H), respectively). Similarly, the EMT status remained the only significant predictor for DFS on multivariate analysis in our cohort. Together, these findings confirm a significant association between PD-L1 and EMT status in PTC.

IFN-γ induced PD-L1 expression and EMT *in vitro*

In order to investigate the relationship between PD-L1 expression and EMT status, PD-L1 expression was induced via IFN-γ treatment in three thyroid cancer cell lines (K1; papillary thyroid cancer, FTC-133; follicular thyroid cancer, 8505C;

anaplastic thyroid cancer). Following treatment, changes in PD-L1, E-cadherin and vimentin protein expression were assessed via western blot. Treatment with 10ng/mL of IFN-γ for 48 hours significantly increased the expression of PD-L1 in all cell lines (Figures 6A, B and C). Upregulation in PD-L1 occurred alongside a significant decrease in E-cadherin and increase in vimentin expression in two of the thyroid cancer cell lines examined (Figures 6A and B). In the 8505C and K1 cell lines, the morphological appearance changed from cobblestone tightly arranged cells (epithelial like) to spindle shaped cells that were widely distributed (mesenchymal like) (Figures 6D and E). These findings were not observed in the FTC cell line. The FTC-133 cell line, which was originally obtained from a lymph node metastasis of a patient with FTC, demonstrates a spindle-shaped morphology at baseline (Figure 6F) as well as strong levels of vimentin expression in untreated cells (Figure 6C). This cell line may therefore possess a more mesenchymal phenotype constitutively and may not be expected to undergo the same morphological changes observed in 8505C and K1 cells. Collectively, these results suggest that IFN-γ treatment promoted PD-L1 expression and induced EMT characteristics in K1 and 8505C cells.

Discussion:

The significant role of the PD-1/PD-L1 pathway in suppressing the anti-tumour immune response has been well established (30). Immunotherapies targeting the PD-1/PD-L1 axis have exhibited durable responses and improved survival rates across numerous cancer types (31). However, a large fraction of patients still fail to benefit from treatment, with response rates of less than 20% often reported (32). The evaluation of PD-L1 expression via IHC is currently the most widely implemented

tool used in the selection of patients for treatment with PD-1/PD-L1 directed immunotherapies (33). Several concerns regarding its use have been recognised, including inconsistencies in expression between archival versus fresh biopsy, inter- and intratumoural heterogeneity and a lack of standardisation between assays (34). Moreover, response rates of 11 to 20% have been reported in patients with negative PD-L1 expression, highlighting its limited use as an independent biomarker for immunotherapy response (35).

The incorporation of additional predictive markers may improve patient selection and prevent avoidable toxicities and costs in individuals unlikely to benefit from treatment. EMT status has recently been identified as a potential candidate marker that can be implemented alongside PD-L1 to predict patient outcomes and response to therapy (36). Positive PD-L1 expression was significantly associated with the presence of EMT in the tumour tissues from 50 patients diagnosed with head and neck squamous cell carcinoma (19). Overall survival was significantly reduced in PD-L1 positive patients also demonstrating EMT features; these findings were confirmed in an independent validation cohort and two public databases. Similar findings have been observed in non-small-cell lung carcinoma (NSCLC) (37), thymic carcinoma (38), extrahepatic cholangiocarcinoma (39), oral squamous cell carcinoma (40), oesophageal squamous cell carcinoma (OSCC) (41) and hepatocellular carcinoma (42). We have also determined that PTC patients exhibiting a mesenchymal phenotype were more likely to co-express tumoural PD-L1 (p = 0.012). These findings were confirmed in the TCGA dataset analysis, in which a moderate positive linear relationship between EMT status and PD-L1 expression (r = 0.481171) as well as an IFN gene signature (r = 0.360384) was observed. In the

subset of PTCs which experienced disease recurrence/progression (n=40), a stronger correlation was identified between positive PD-L1 and EMT expression (r = 0.623002); this was further strengthened when patients of all subtypes were included in the analysis (n=49) (r = 0.656826). PD-L1, EMT status and CD8 T cell expression were all not significantly associated with any clinicopathological characteristics; this may be a consequence of the relatively small cohort size, and the limited number of patients presenting with metastatic disease. EMT status remained the only significant predictor of DFS on multivariate analysis (p = 0.032); these findings were also reflected in the TCGA PTC patient cohort, in which a higher EMT and mesenchymal genes score were both significantly associated with a poorer DFS (p = 0.0027 and p = 0.0085, respectively).

The mechanisms by which EMT regulates components of the tumour immune microenvironment, including the PD-1/PD-L1 pathway, have recently been elucidated. A meta-analysis revealed that *PD-L1* gene expression was co-amplified along with the EMT associated genes *MYC, SOX2, N-cadherin* and *SNAI1* in the endometrial and ovarian cancer datasets from TCGA (43). The gene promoter region of PD-L1 contains a binding site for ZEB1, a transcription factor which contributes to cancer stemness and tumourigenesis (44, 45). siRNA-mediated ZEB1 knockdown suppressed PD-L1 levels whilst promoting E-cadherin expression in OSCC (46). Cases expressing high PD-L1 at the invasive front also had significantly greater tumour invasion, EMT, and less CD8 lymphocyte infiltration. EMT-converted OSCC cell lines expressing high levels of PD-L1 at both protein and mRNA levels were capable of inducing T-cell apoptosis to a greater extent when compared to the original epithelial type tumour cells (41). In breast cancer cell lines, EMT-mediated

PD-L1 upregulation occurred in parallel with the up- and down-regulation of the stem-cell-related CD44 and CD24 surface markers, respectively; this was also accompanied by a morphological change from tightly arranged epithelial-like cells to widely distributed mesenchymal-like cells (22). A molecular relationship between EMT and CD8 T cells was demonstrated by Chen et al., in which ZEB1, an EMT activator and transcriptional repressor of miR-200 (a cell-autonomous suppressor of EMT and metastasis), was shown to relieve miR-200 repression of PD-L1 on tumour cells, resulting in CD8 T-cell immunosuppression and metastasis. These findings were further supported by a strong correlation between EMT score, levels of miR-200 and PD-L1 expression in numerous human lung cancer datasets. Preclinical models of melanoma, pancreatic and breast cancer have also demonstrated that the expression of certain transcription factors, such as Snail or Neu, can induce EMT and are associated with the activation of immunosuppressive cytokines and T-cell resistance. In our study, the prognostic capabilities of EMT were markedly enhanced when used in conjunction with PD-L1 and CD8 expression ($p < 0.0001$). Additional prospective studies exploring the interplay between CD8 T cells, EMT and PD-L1 in larger patient cohorts will be needed to confirm these findings.

PD-1/PD-L1 oncogenic signalling has also been shown to play an important role in the regulation of EMT. Atezolizumab, an anti-PD-L1 checkpoint inhibitor, was shown to downregulate genes promoting cell migration, invasion and metastasis in the human triple negative breast cancer cell line MDA-MB-231 (47). In human glioblastoma multiform (GBM) cells, PD-L1 significantly altered cell growth, migration and invasion pathways by upregulating N-cadherin, vimentin, Slug (an E-cadherin transcriptional suppressor) and β-catenin (activates EMT via the PI3K/Akt/mTOR

pathway), and downregulating E-cadherin gene expression (48). PD-L1 overexpression promoted GBM development and invasion in orthotopic GBM rat models. Following 48 hours of IFN-γ treatment, we also detected a significant increase in PD-L1 expression in all thyroid cancer cell lines examined. This rise in PD-L1 was accompanied by phenotypic changes indicative of a mesenchymal phenotype on imaging. This was confirmed on western blot, where a significant downregulation in E-cadherin expression and upregulation of vimentin levels was observed. Similar findings were reported by Lo et al., in which IFNs enhanced RCC invasiveness by increasing both Slug and ZEB1 gene expression (49). IFN-γ induced PD-L1 upregulation may therefore be involved in promoting EMT and may prove to be the missing link in the treatment of mesenchymal cancers. Collectively, these studies illuminate the complex bidirectional regulation between EMT and PD-L1 signalling in cancer which ultimately leads to tumour immune escape and invasion.

Interestingly, an integrated analysis of the genomic and proteomic profiles from over 1,000 tumours revealed that additional targetable immune checkpoints are present in cancers displaying an EMT phenotype, including T-cell immunoglobulin and mucin-domain containing-3 (TIM-3), OX40 and cytotoxic T-lymphocyte-associated protein 4 (CTLA-4) (50). EMT may therefore accelerate cancer growth and metastasis not only through the direct reprogramming of the PD-1/PD-L1 axis, but also via the modulation of several immune processes within the tumour microenvironment. This finding highlights the possibility of utilising EMT status as a supplementary tool for the selection of patients who may benefit from immune checkpoint inhibitors. Therapies targeting these additional immune checkpoints may impede tumour metastases and drug resistance mediated via EMT.

EMT status has also been shown to influence the degree of response to PD-1/PD-L1 targeted immunotherapies. Mammary tumour cells arising from epithelial carcinoma cell lines were found to express lower levels of PD-L1 and elevated MHC-I, CD8 T cells and M1 (anti-tumour) macrophages (51). In contrast, tumours from more-mesenchymal carcinoma cell lines exhibited low levels of MHC-I and an elevated expression EMT markers, PD-L1, regulatory T cells, M2 (pro-tumour) macrophages and exhausted CD8 T cells within their stroma. The more mesenchymal carcinoma cells within a tumour were able to safeguard their more epithelial counterparts from immune attack, implicating the role of EMT in the regulation of the tumour microenvironment. Moreover, epithelial tumours were more susceptible to elimination by immunotherapy than corresponding mesenchymal tumours. Therefore, the implementation of EMT inhibitors as adjuvants to immune checkpoint immunotherapies may enhance responses in patients with mesenchymal tumours. In patients with advanced melanoma, EMT signatures and mesenchymal-related genes were associated with innate anti-PD-1 resistance (52). Additionally, patients with bladder tumours characterised by an epithelial phenotype had significantly higher response rates following treatment with atezolizumab therapy compared to those harbouring a basal subtype (53). M7824, a novel first-in-class bifunctional anti-PD-L1 and TGF-β fusion protein, was shown to revert TGF-β mediated mesenchymalisation in NSCLC cells, as well as promote the activation of CD8 T and NK cells, reduce tumour growth and extend survival in animal models of colon and breast cancer. The concurrent blockade of the PD-L1 and TGF-β pathways elicited superior antitumour activity compared to either monotherapy alone. These findings suggest that the efficacy of anti-PD-1/PD-L1 checkpoint inhibitors

may be influenced by an individual's EMT status. Additional trials investigating the efficacy of combination strategies comprised of EMT targeted agents and immune checkpoint inhibitors will be needed to overcome patient resistance and improve survival outcomes.

In conclusion, our results reveal the significant prognostic capabilities of PD-L1 expression, CD8 T cell status and EMT in PTC. Moreover, we provide a feasible mechanism for the promotion of EMT in thyroid cells that is mediated by PD-L1 expression *in vitro*. Patients exhibiting an EMT phenotype and positive PD-L1 expression may benefit from PD-1/PD-L1 targeted immunotherapy. Additional research exploring the molecular mechanisms underlying EMT regulation and its association with the PD-1/PD-L1 axis will enhance our understanding of thyroid carcinogenesis and provide alternative approaches for the treatment of patients with aggressive disease.

Figure legends:

Figure 1: Representative staining of formalin-fixed paraffin-embedded (FFPE) tissues from PTC patients. Negative **(A)** and Positive **(B)** immunohistochemical (IHC) staining pattern for E-cadherin expression. Negative **(C)** and Positive **(D)** IHC staining pattern for vimentin expression. Negative **(E)** and positive **(F)** IHC staining pattern for PD-L1 expression. Negative **(G)** and positive **(H)** IHC staining pattern for $CD8^+$ expression. Images were taken at 5x magnification (Figure A) and 40x magnification (remaining images).

Figure 2: PD-L1 expression is associated with mesenchymal phenotype. Cases were separated in PD-L1 negative (blue) (n=25) and positive (red) (n=49) subgroups. These were then assessed for epithelial vs. mesenchymal state. By Fisher's exact test there was a significant positive association between PD-L1 expression and a mesenchymal phenotype.

Figure 3: Vimentin, $CD8^+$ and PD-L1 were all predictive for DFS in the PTC cohort. Kaplan-Meier curves for DFS of PTC patients with positive and negative E-cadherin expression ($E\text{-}cad^{pos}$ (n=16) vs. $E\text{-}cad^{neg}$ (n=58); p = 0.384) **(A)**, vimentin expression ($Vimentin^{pos}$ (n=51) vs. $Vimentin^{neg}$ (n=23); p = 0.003) **(B)**, $CD8^+$ density ($CD8^{pos}$ (n=39) vs. $CD8^{neg}$ (n=35); p = 0.028) **(C)** and positive or negative PD-L1 expression ($PD\text{-}L1^{pos}$ (n=49) vs. $PD\text{-}L1^{neg}$ (n=25); p = 0.048) **(D)**. p-values were calculated by the log-rank test.

Figure 4: Patients positive for EMT and PD-L1 expression, and negative for $CD8^+$ T-cell expression experienced the worst DFS on subgroup analysis. Kaplan-Meier curves for DFS of PTC patients with positive and negative E-cadherin and Vimentin expression ($E\text{-}cad^{neg}/Vim^{neg}$ (n=13) vs. $E\text{-}cad^{pos}/Vim^{neg}$ (n=10) vs. $E\text{-}cad^{neg}/Vim^{pos}$ (n=45) vs. $E\text{-}cad^{pos}/Vim^{pos}$ (n=6); p=0.026) **(A)**, positive and negative EMT status and PD-L1 expression ($EMT^{neg}/PD\text{-}L1^{neg}$ (n=39) vs. $EMT^{neg}/PD\text{-}L1^{pos}$ and $EMT^{pos}/PD\text{-}L1^{neg}$ and $EMT^{pos}/PD\text{-}L1^{pos}$ (n=35); p=0.003) **(B)**, and positive and negative EMT status, PD-L1 expression and CD8 density ($EMT^{pos}/PD\text{-}L1^{pos}/CD8^{neg}$ (n=15) vs. $EMT^{neg}/PD\text{-}L1^{neg}/CD8^{pos}$ (n=7) vs. Other (n=52); p<0.0001) **(C)**. p values were calculated by the log-rank test.

Figure 5: Correlation of PD-L1 expression, EMT and an IFN gene signature in thyroid cancer using TCGA gene expression dataset. Gene expression dataset from the TCGA thyroid cancer samples (total of 516 patients) showing the correlation between PD-L1 expression with EMT score (r = 0.481171) **(A)**, correlation between IFN score and EMT score (r = 0.360384) **(B)**. Correlation between PD-L1 expression and EMT score in PTC patients only (n=399) (r = 0.502354) **(C)**. Correlation between PD-L1 expression and EMT score in PTC patients experiencing disease recurrence/progression (n=40) (r = 0.623002) **(D)**. Correlation between PD-L1 expression and EMT score in all patients experiencing disease recurrence/progression (n=49) (r = 0.656826) **(E)**. Heat map showing mRNA expression level of epithelial genes, mesenchymal genes, and IFN-γ related genes **(F)**. Kaplan-Meier curves for DFS of TCGA thyroid cancer patients with positive and negative EMT score ($p = 0.0027$) **(G)** and positive and negative mesenchymal gene expression ($p = 0.0085$) **(H)**.

Figure 6: IFN-γ treatment upregulated PD-L1 expression and induced EMT in thyroid cancer cell lines. PD-L1, E-cadherin and vimentin expression following 48-hour 10 ng/mL IFN-γ treatment in 8505C **(A)**, K1 **(B)** and FTC-133 **(C)** thyroid cancer cells lines. A morphological change indicative of EMT was observed in the 8505C **(D)** and K1 **(E)** cell lines. This was not evident in the FTC **(F)** cell line which demonstrated a more mesenchymal morphology at baseline. Quantification of western blotting data (n=3) was performed via Licor Odyssey, which showed a significant reduction in PD-L1 expression in all cell lines assessed. *p* values were calculated by the student t test. *$p < 0.05$, **$p < 0.01$. All experiments were performed in triplicate.

List of abbreviations:

AJCC: American Joint Committee on Cancer

ATA: American Thyroid Association

ATC: Anaplastic thyroid cancer

CONCERT: Centre for Oncology Education and Research Translation

CTLA-4: Cytotoxic T-lymphocyte-associated protein 4

DFS: Disease-free survival

DTC: Differentiated thyroid cancer

EMT: Epithelial-to-mesenchymal transition

EpCAM: Epithelial cell adhesion molecule

FBS: Foetal bovine serum

FFPE: Formalin-fixed paraffin-embedded

FTC: Follicular thyroid cancer

GBM: Glioblastoma multiform

IFN: Interferon

IHC: Immunohistochemical

NSCLC: Non-small-cell lung carcinoma

OSCC: Oesophageal squamous cell carcinoma

PD-1: Programmed cell death protein 1

PD-L1: Programmed death ligand 1

PD-L2: Programmed death ligand 2

RAI: Radioactive iodine

TCGA: The Cancer Genome Atlas

Tg: Thyroglobulin

TIM-3: T-cell immunoglobulin and mucin-domain containing-3

TMA: Tissue microarrays

TNM: Tumour node metastasis

TSH: Thyroid stimulating hormone

UICC: Union against Cancer

Declarations:

Ethics approval and consent to participate:

Ethics approval was obtained from the South West Sydney Local Health District Human Research Ethics Committee via the Centre for Oncology Education and Research Translation (CONCERT) Biobank, Australia/TCRC/3/02- 03-2015.

Consent for publication:

Not applicable

Availability of data and materials:

Not applicable

Competing interests:

Not applicable

Funding:

TLR is supported by a CINSW Future Research Leader fellowship and funding from the CONCERT translational cancer research centre. AJ is supported by funding from Liverpool Hospital Medical Oncology and Clinical Trials Unit. MJA is supported by a Western Sydney University PhD scholarship. US holds a Fellowship from the Cancer

Institute of New South Wales. Financial support was provided by the Cancer Council NSW (RG20-12) to US.

Author's contributions:

MJA constructed the TMAs, analysed and interpreted the patient data, performed the *in vitro* experiments and was a major contributor in writing the manuscript. TY analysed and interpreted the TMAs and was a major contributor in writing the manuscript. US performed all of the clinical dataset analysis and was a major contributor in writing the manuscript. AJ assisted in completing the *in vitro* experimentation and interpretation and was a major contributor in writing the manuscript. CEM assisted in analysing and interpreting the patient data and was a major contributor in writing the manuscript. PS, NN and TLR made significant contributions to the conception and design of the research, acquisition of patient samples, and in writing and editing the manuscript. All authors read and approved the final manuscript.

Acknowledgements:

Not applicable

References:

1. Morris LGT, Sikora AG, Tosteson TD, Davies L. The increasing incidence of thyroid cancer: the influence of access to care. Thyroid : official journal of the American Thyroid Association. 2013;23(7):885-91.

2. Sherman SI. Thyroid carcinoma. Lancet (London, England). 2003;361(9356):501-11.
3. Pellegriti G, Frasca F, Regalbuto C, Squatrito S, Vigneri R. Worldwide increasing incidence of thyroid cancer: update on epidemiology and risk factors. Journal of cancer epidemiology. 2013;2013:965212.
4. Leux C, Guenel P. Risk factors of thyroid tumors: role of environmental and occupational exposures to chemical pollutants. Revue d'epidemiologie et de sante publique. 2010;58(5):359-67.
5. Kim H, Kim HI, Kim SW, Jung J, Jeon MJ, Kim WG, et al. Prognosis of Differentiated Thyroid Carcinoma with Initial Distant Metastasis: A Multicenter Study in Korea. Endocrinol Metab (Seoul). 2018;33(2):287-95.
6. Parameswaran R, Shulin Hu J, Min En N, Tan WB, Yuan NK. Patterns of metastasis in follicular thyroid carcinoma and the difference between early and delayed presentation. Ann R Coll Surg Engl. 2017;99(2):151-4.
7. Durante C, Haddy N, Baudin E, Leboulleux S, Hartl D, Travagli JP, et al. Long-term outcome of 444 patients with distant metastases from papillary and follicular thyroid carcinoma: benefits and limits of radioiodine therapy. The Journal of clinical endocrinology and metabolism. 2006;91(8):2892-9.
8. Ross DS. Predicting Outcome in Patients with Thyroid Cancer. The Journal of Clinical Endocrinology & Metabolism. 2013;98(12):4673-5.
9. Francisco LM, Sage PT, Sharpe AH. The PD-1 pathway in tolerance and autoimmunity. Immunol Rev. 2010;236:219-42.
10. Francisco LM, Sage PT, Sharpe AH. The PD-1 pathway in tolerance and autoimmunity. Immunol Rev. 2010;236:219-42.

11. Jiang X, Wang J, Deng X, Xiong F, Ge J, Xiang B, et al. Role of the tumor microenvironment in PD-L1/PD-1-mediated tumor immune escape. Molecular cancer. 2019;18(1):10-.

12. Pyo JS, Kang G, Kim JY. Prognostic role of PD-L1 in malignant solid tumors: a meta-analysis. The International journal of biological markers. 2017;32(1):e68-e74.

13. Aghajani M, Graham S, McCafferty C, Shaheed CA, Roberts T, DeSouza P, et al. Clinicopathologic and Prognostic Significance of Programmed Cell Death Ligand 1 Expression in Patients with Non-Medullary Thyroid Cancer: A Systematic Review and Meta-Analysis. Thyroid : official journal of the American Thyroid Association. 2018;28(3):349-61.

14. Shen X, Zhao B. Efficacy of PD-1 or PD-L1 inhibitors and PD-L1 expression status in cancer: meta-analysis. BMJ. 2018;362:k3529.

15. Mehnert JM, Varga A, Brose MS, Aggarwal RR, Lin CC, Prawira A, et al. Safety and antitumor activity of the anti-PD-1 antibody pembrolizumab in patients with advanced, PD-L1-positive papillary or follicular thyroid cancer. BMC cancer. 2019;19(1):196.

16. Spencer KR, Wang J, Silk AW, Ganesan S, Kaufman HL, Mehnert JM. Biomarkers for Immunotherapy: Current Developments and Challenges. American Society of Clinical Oncology Educational Book. 2016(36):e493-e503.

17. Kalluri R, Neilson EG. Epithelial-mesenchymal transition and its implications for fibrosis. The Journal of clinical investigation. 2003;112(12):1776-84.

18. Satelli A, Li S. Vimentin in cancer and its potential as a molecular target for cancer therapy. Cellular and molecular life sciences : CMLS. 2011;68(18):3033-46.

780 19. Ock C-Y, Kim S, Keam B, Kim M, Kim TM, Kim J-H, et al. PD-L1 expression is
781 associated with epithelial-mesenchymal transition in head and neck squamous cell
782 carcinoma. Oncotarget. 2016;7(13):15901-14.
783 20. Soundararajan R, Fradette JJ, Konen JM, Moulder S, Zhang X, Gibbons DL,
784 et al. Targeting the Interplay between Epithelial-to-Mesenchymal-Transition and the
785 Immune System for Effective Immunotherapy. Cancers (Basel). 2019;11(5):714.
786 21. Lou Y, Diao L, Cuentas ER, Denning WL, Chen L, Fan YH, et al. Epithelial-
787 Mesenchymal Transition Is Associated with a Distinct Tumor Microenvironment
788 Including Elevation of Inflammatory Signals and Multiple Immune Checkpoints in
789 Lung Adenocarcinoma. Clinical cancer research : an official journal of the American
790 Association for Cancer Research. 2016;22(14):3630-42.
791 22. Alsuliman A, Colak D, Al-Harazi O, Fitwi H, Tulbah A, Al-Tweigeri T, et al.
792 Bidirectional crosstalk between PD-L1 expression and epithelial to mesenchymal
793 transition: significance in claudin-low breast cancer cells. Mol Cancer. 2015;14:149.
794 23. Maleki Vareki S. High and low mutational burden tumors versus
795 immunologically hot and cold tumors and response to immune checkpoint inhibitors.
796 Journal for ImmunoTherapy of Cancer. 2018;6(1):157.
797 24. Caixeiro NJ, Morteza A, de Souza P, Lee CS. The Centre for Oncology
798 Education and Research Translation (CONCERT) Biobank. Open Journal of
799 Bioresources. 2015 2(1):p.Art.e3. doi:http://dx.doi.org/10.5334/ojb.ai.
800 25. Caixeiro NJ, Aghmesheh, M., de Souza, P., & Lee, C. S. (2015). The Centre
801 for Oncology Education and Research Translation (CONCERT) Biobank. Open
802 Journal of Bioresources, 2(1), Art. e3. DOI: http://doi.org/10.5334/ojb.ai.
803 26. Haugen BR, Alexander EK, Bible KC, Doherty GM, Mandel SJ, Nikiforov YE,
804 et al. 2015 American Thyroid Association Management Guidelines for Adult Patients

805 with Thyroid Nodules and Differentiated Thyroid Cancer: The American Thyroid
806 Association Guidelines Task Force on Thyroid Nodules and Differentiated Thyroid
807 Cancer. Thyroid : official journal of the American Thyroid Association. 2016;26(1):1-
808 133.
809 27. Aghajani MJ, Yang T, McCafferty CE, Graham S, Wu X, Niles N. Predictive
810 relevance of programmed cell death protein 1 and tumor-infiltrating lymphocyte
811 expression in papillary thyroid cancer. Surgery. 2018;163(1):130-6.
812 28. Roberts TL, Ho U, Luff J, Lee CS, Apte SH, MacDonald KP, et al. Smg1
813 haploinsufficiency predisposes to tumor formation and inflammation. Proc Natl Acad
814 Sci U S A. 2013;110(4):E285-94.
815 29. Gu Z, Eils R, Schlesner M. Complex heatmaps reveal patterns and
816 correlations in multidimensional genomic data. Bioinformatics (Oxford, England).
817 2016;32(18):2847-9.
818 30. Topalian SL, Drake CG, Pardoll DM. Targeting the PD-1/B7-H1(PD-L1)
819 pathway to activate anti-tumor immunity. Current opinion in immunology.
820 2012;24(2):207-12.
821 31. Wu X, Gu Z, Chen Y, Chen B, Chen W, Weng L, et al. Application of PD-1
822 Blockade in Cancer Immunotherapy. Computational and structural biotechnology
823 journal. 2019;17:661-74.
824 32. Sharma P, Hu-Lieskovan S, Wargo JA, Ribas A. Primary, Adaptive, and
825 Acquired Resistance to Cancer Immunotherapy. Cell. 2017;168(4):707-23.
826 33. Gibney GT, Weiner LM, Atkins MB. Predictive biomarkers for checkpoint
827 inhibitor-based immunotherapy. The Lancet Oncology. 2016;17(12):e542-e51.
828 34. Buttner R, Gosney JR, Skov BG, Adam J, Motoi N, Bloom KJ, et al.
829 Programmed Death-Ligand 1 Immunohistochemistry Testing: A Review of Analytical

Assays and Clinical Implementation in Non-Small-Cell Lung Cancer. Journal of clinical oncology : official journal of the American Society of Clinical Oncology. 2017;35(34):3867-76.

35. Prelaj A, Tay R, Ferrara R, Chaput N, Besse B, Califano R. Predictive biomarkers of response for immune checkpoint inhibitors in non-small-cell lung cancer. European journal of cancer (Oxford, England : 1990). 2019;106:144-59.

36. Terry S, Savagner P, Ortiz-Cuaran S, Mahjoubi L, Saintigny P, Thiery J-P, et al. New insights into the role of EMT in tumor immune escape. Mol Oncol. 2017;11(7):824-46.

37. Asgarova A, Asgarov K, Godet Y, Peixoto P, Nadaradjane A, Boyer-Guittaut M, et al. PD-L1 expression is regulated by both DNA methylation and NF-kB during EMT signaling in non-small cell lung carcinoma. Oncoimmunology. 2018;7(5):e1423170.

38. Funaki S, Shintani Y, Fukui E, Yamamoto Y, Kanzaki R, Ose N, et al. The prognostic impact of programmed cell death 1 and its ligand and the correlation with epithelial-mesenchymal transition in thymic carcinoma. Cancer Med. 2019;8(1):216-26.

39. Ueno T, Tsuchikawa T, Hatanaka KC, Hatanaka Y, Mitsuhashi T, Nakanishi Y, et al. Prognostic impact of programmed cell death ligand 1 (PD-L1) expression and its association with epithelial-mesenchymal transition in extrahepatic cholangiocarcinoma. Oncotarget. 2018;9(28):20034-47.

40. Hirai M, Kitahara H, Kobayashi Y, Kato K, Bou-Gharios G, Nakamura H, et al. Regulation of PD-L1 expression in a high-grade invasive human oral squamous cell carcinoma microenvironment. Int J Oncol. 2017;50(1):41-8.

41. Thar Min AK, Okayama H, Saito M, Ashizawa M, Aoto K, Nakajima T, et al. Epithelial-mesenchymal transition-converted tumor cells can induce T-cell apoptosis through upregulation of programmed death ligand 1 expression in esophageal squamous cell carcinoma. Cancer Med. 2018.

42. Shrestha R, Prithviraj P, Anaka M, Bridle KR, Crawford DHG, Dhungel B, et al. Monitoring Immune Checkpoint Regulators as Predictive Biomarkers in Hepatocellular Carcinoma. Front Oncol. 2018;8:269-.

43. Dong P, Xiong Y, Yue J, Hanley SJB, Watari H. Tumor-Intrinsic PD-L1 Signaling in Cancer Initiation, Development and Treatment: Beyond Immune Evasion. Front Oncol. 2018;8:386-.

44. Rosenbloom KR, Armstrong J, Barber GP, Casper J, Clawson H, Diekhans M, et al. The UCSC Genome Browser database: 2015 update. Nucleic acids research. 2015;43(Database issue):D670-81.

45. Sánchez-Tilló E, Siles L, de Barrios O, Cuatrecasas M, Vaquero EC, Castells A, et al. Expanding roles of ZEB factors in tumorigenesis and tumor progression. Am J Cancer Res. 2011;1(7):897-912.

46. Tsutsumi S, Saeki H, Nakashima Y, Ito S, Oki E, Morita M, et al. Programmed death-ligand 1 expression at tumor invasive front is associated with epithelial-mesenchymal transition and poor prognosis in esophageal squamous cell carcinoma. Cancer Sci. 2017;108(6):1119-27.

47. Saleh R, Taha RZ, Sasidharan Nair V, Alajez NM, Elkord E. PD-L1 Blockade by Atezolizumab Downregulates Signaling Pathways Associated with Tumor Growth, Metastasis, and Hypoxia in Human Triple Negative Breast Cancer. Cancers (Basel). 2019;11(8).

878 48. Qiu XY, Hu DX, Chen WQ, Chen RQ, Qian SR, Li CY, et al. PD-L1 confers
879 glioblastoma multiforme malignancy via Ras binding and Ras/Erk/EMT activation.
880 Biochimica et biophysica acta Molecular basis of disease. 2018;1864(5 Pt A):1754-
881 69.
882 49. Lo UG, Bao J, Cen J, Yeh H-C, Luo J, Tan W, et al. Interferon-induced IFIT5
883 promotes epithelial-to-mesenchymal transition leading to renal cancer invasion. Am J
884 Clin Exp Urol. 2019;7(1):31-45.
885 50. Mak MP, Tong P, Diao L, Cardnell RJ, Gibbons DL, William WN, et al. A
886 Patient-Derived, Pan-Cancer EMT Signature Identifies Global Molecular Alterations
887 and Immune Target Enrichment Following Epithelial-to-Mesenchymal Transition.
888 Clinical cancer research : an official journal of the American Association for Cancer
889 Research. 2016;22(3):609-20.
890 51. Dongre A, Rashidian M, Reinhardt F, Bagnato A, Keckesova Z, Ploegh HL, et
891 al. Epithelial-to-Mesenchymal Transition Contributes to Immunosuppression in
892 Breast Carcinomas. Cancer research. 2017;77(15):3982-9.
893 52. Hugo W, Zaretsky JM, Sun L, Song C, Moreno BH, Hu-Lieskovan S, et al.
894 Genomic and Transcriptomic Features of Response to Anti-PD-1 Therapy in
895 Metastatic Melanoma. Cell. 2016;165(1):35-44.
896 53. Rosenberg JE, Hoffman-Censits J, Powles T, van der Heijden MS, Balar AV,
897 Necchi A, et al. Atezolizumab in patients with locally advanced and metastatic
898 urothelial carcinoma who have progressed following treatment with platinum-based
899 chemotherapy: a single-arm, multicentre, phase 2 trial. Lancet (London, England).
900 2016;387(10031):1909-20.
901

Figures

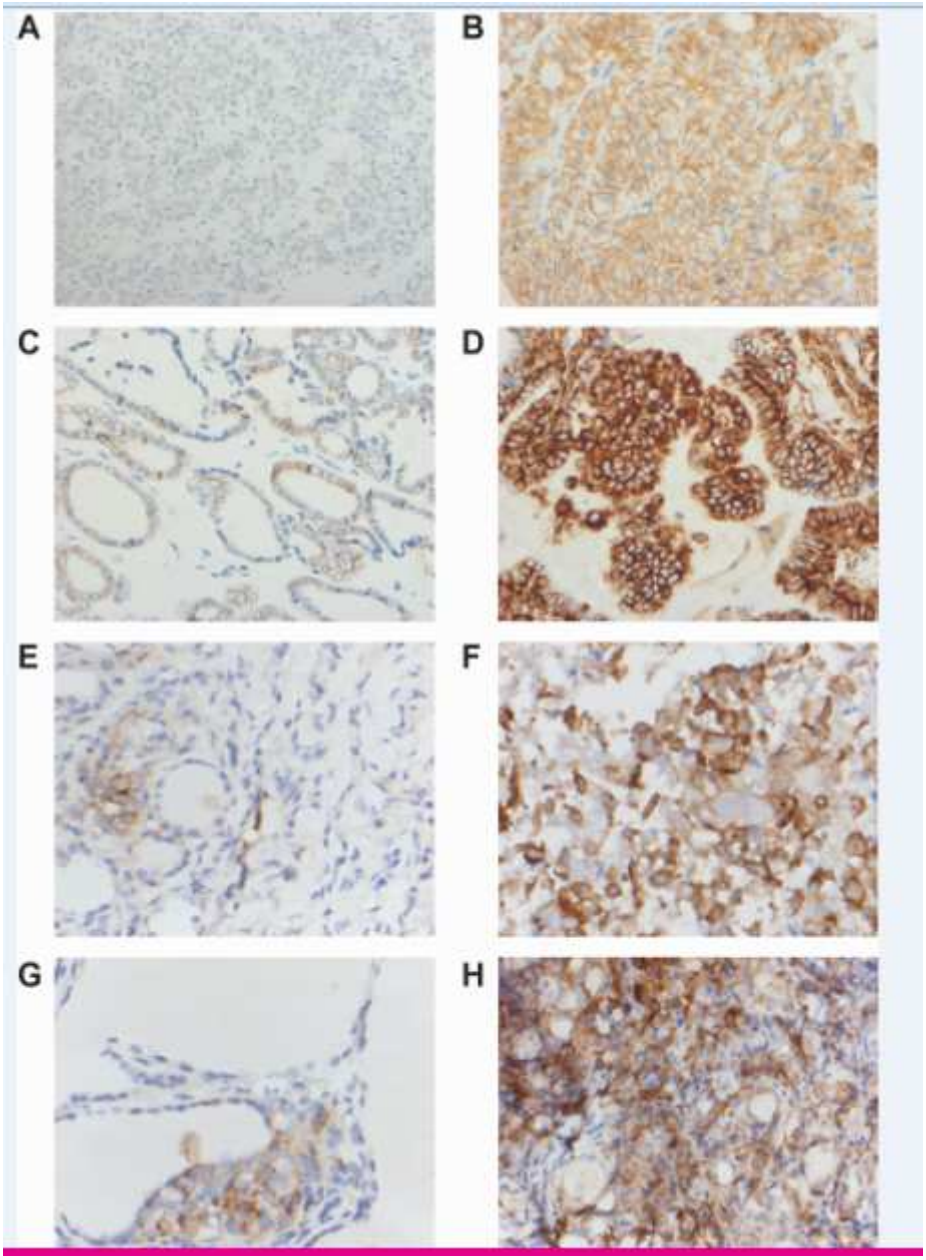

Figure 1

[Please see the manuscript to view the figure caption.]

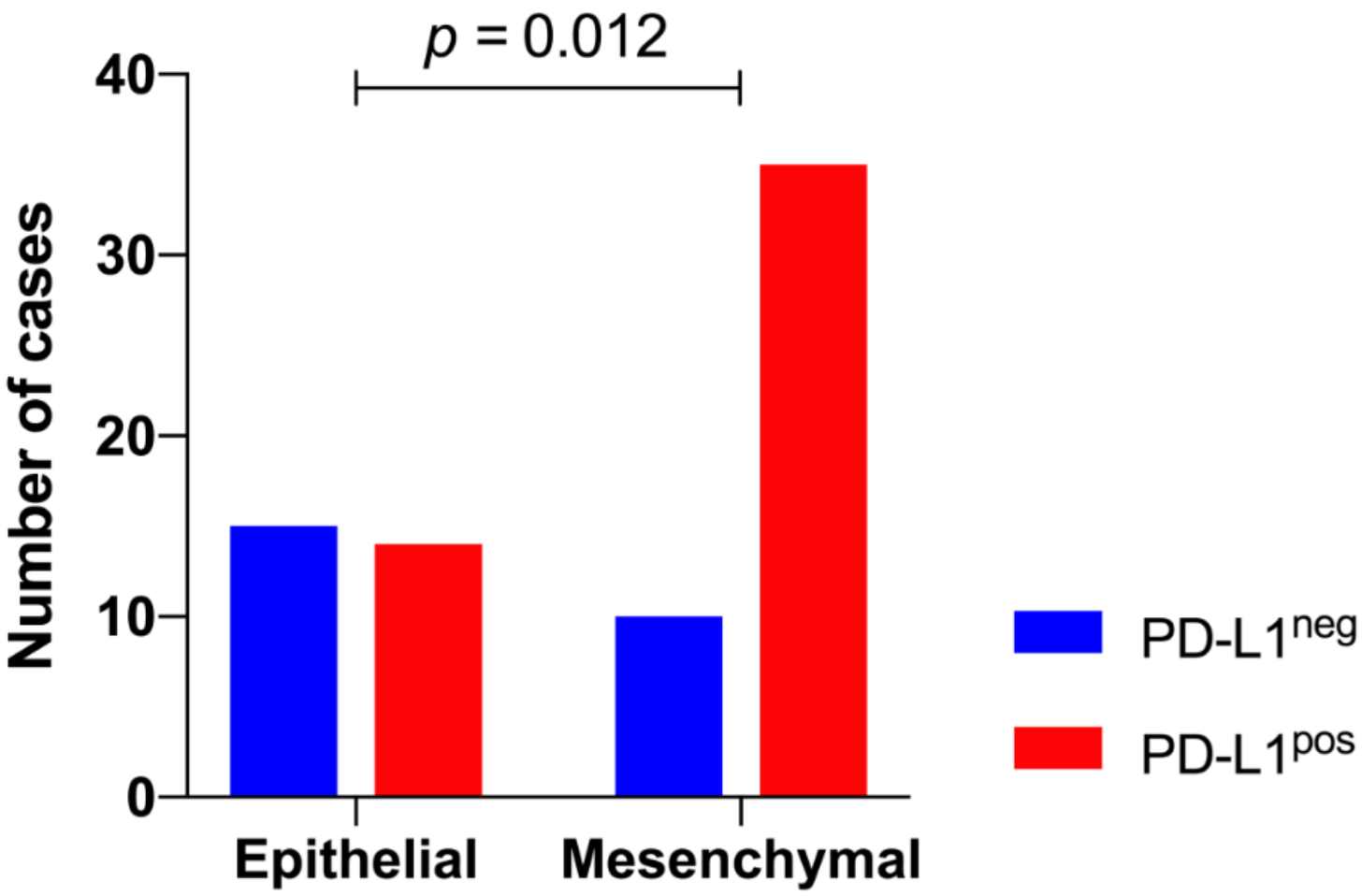

Figure 2

[Please see the manuscript to view the figure caption.]

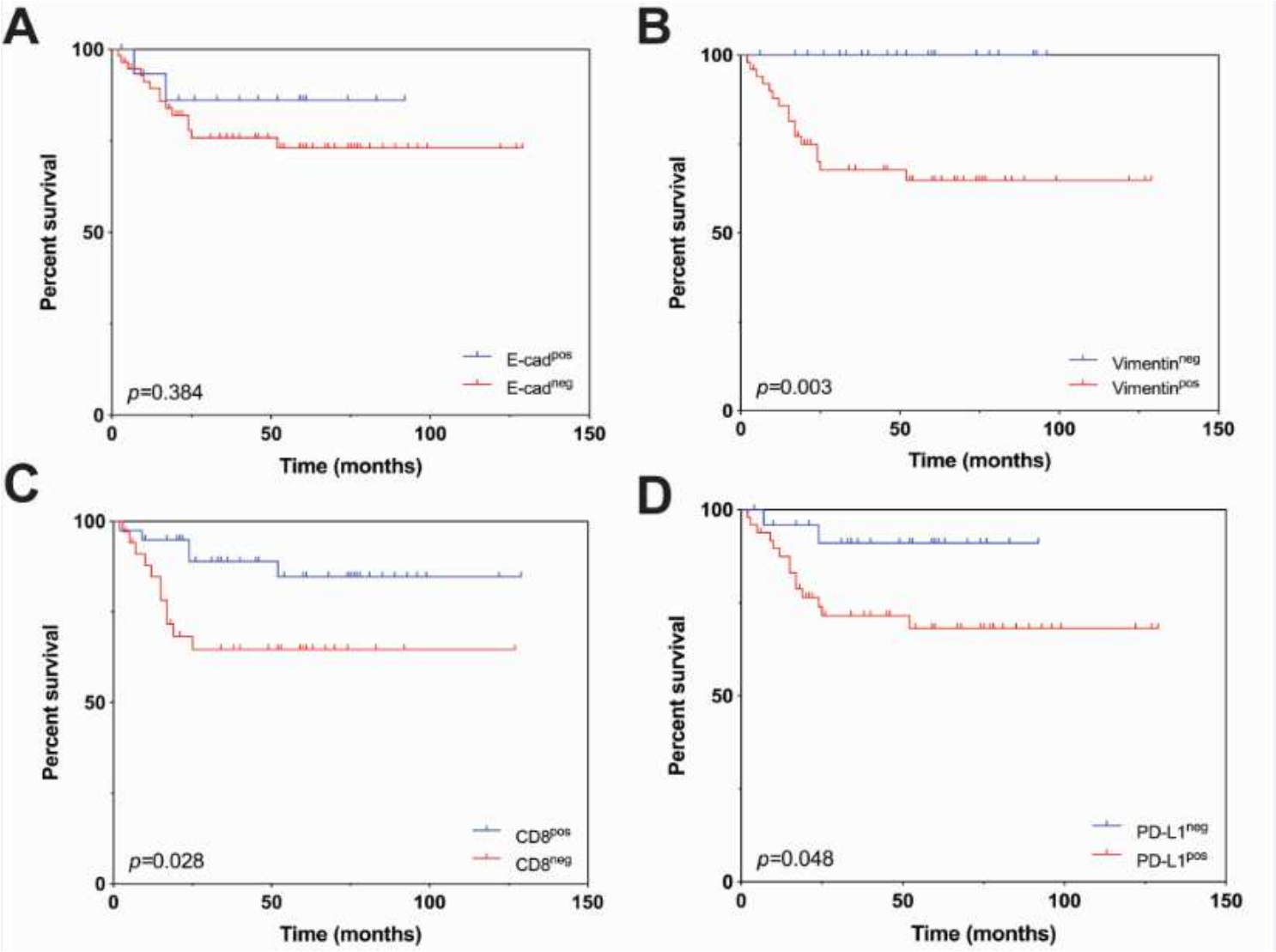

Figure 3

[Please see the manuscript to view the figure caption.]

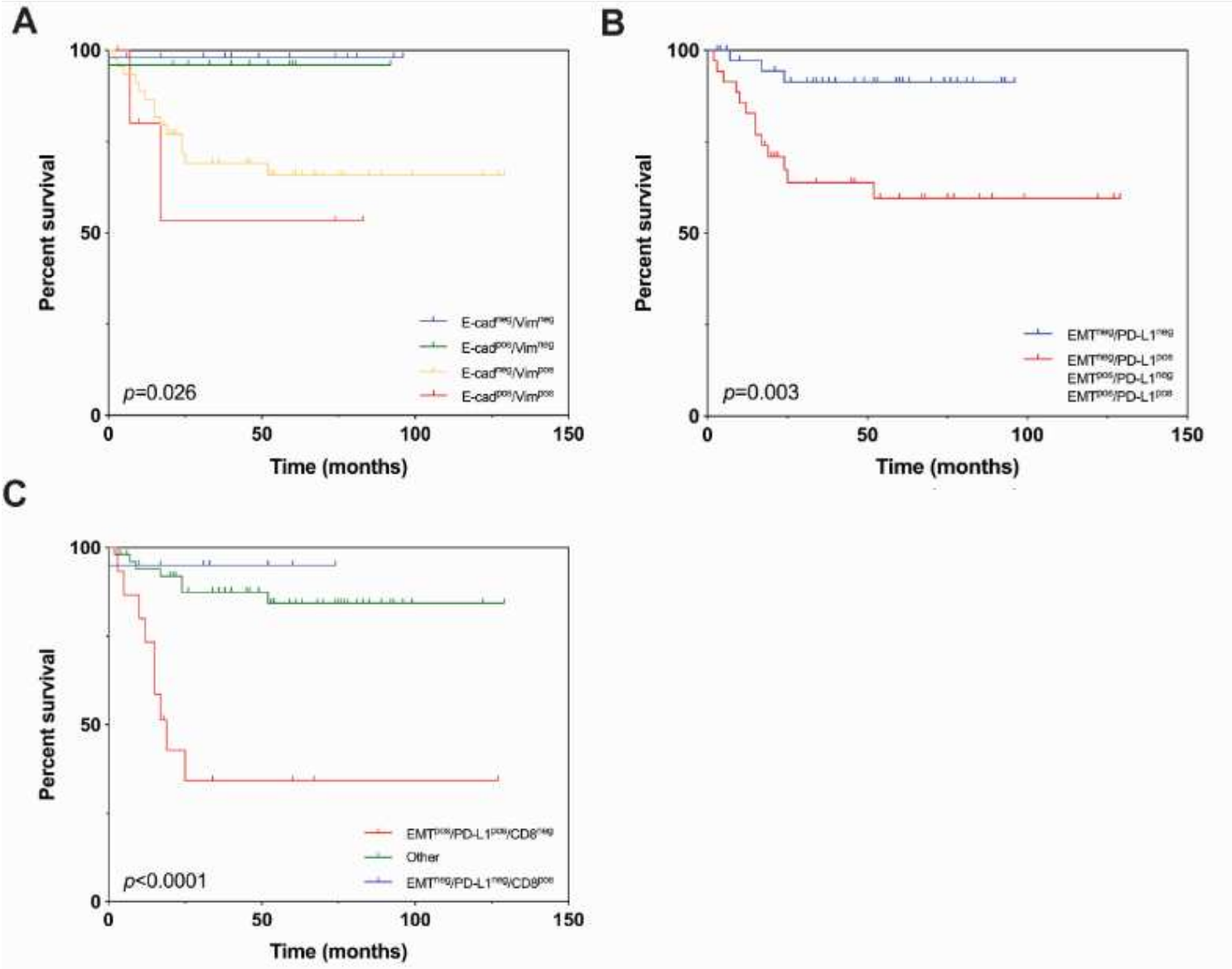

Figure 4

[Please see the manuscript to view the figure caption.]

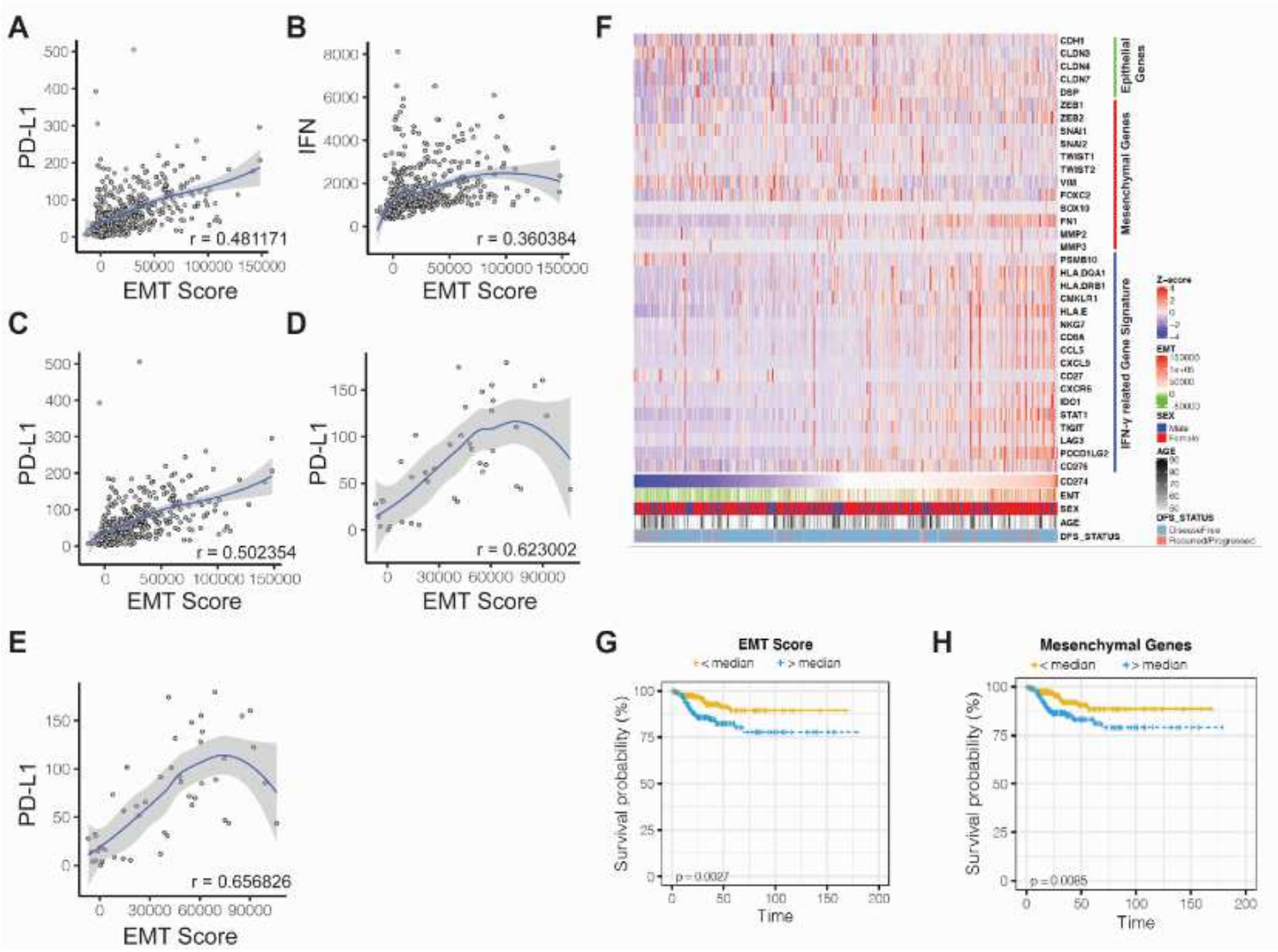

Figure 5

[Please see the manuscript to view the figure caption.]

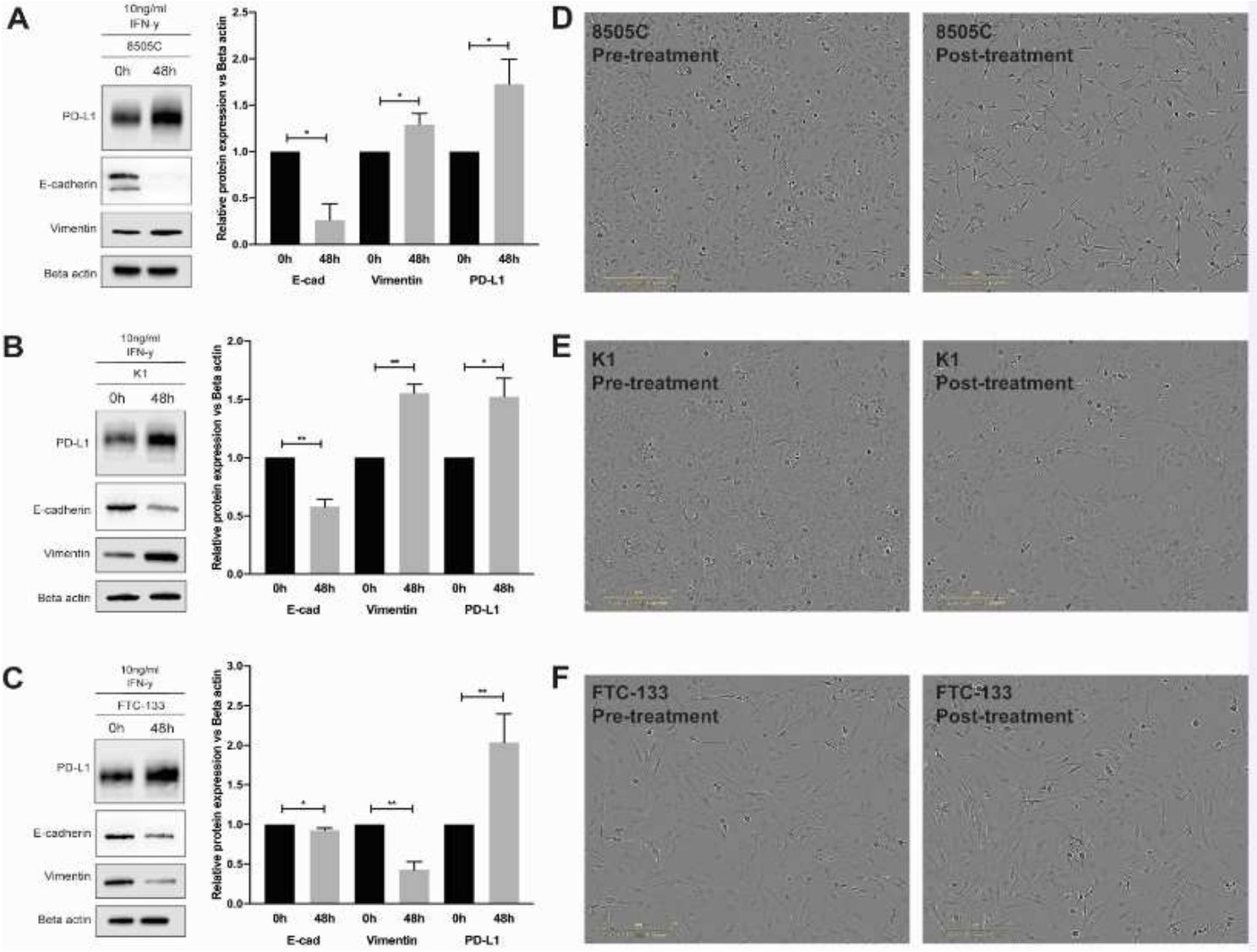

Figure 6

[Please see the manuscript to view the figure caption.]

Supplementary Files

This is a list of supplementary files associated with this preprint. Click to download.

- SupplementaryTables.pdf
- SupplementaryTables.pdf